energies

MDPI

Article

Preliminary Techno-Economic Study of Optimized Floating Offshore Wind Turbine Substructure

Adebayo Ojo [1,*], Maurizio Collu [1] and Andrea Coraddu [2]

[1] Department of Naval Architecture Ocean and Marine Engineering, University of Strathclyde, Glasgow G4 0LZ, UK; maurizio.collu@strath.ac.uk
[2] Department of Maritime & Transport Technology, Delft University of Technology, 2628 CD Delft, The Netherland; a.coraddu@tudelft.nl
* Correspondence: adebayo.ojo@strath.ac.uk

Abstract: Floating offshore wind turbines (FOWTs) are still in the pre-commercial stage and, although different concepts of FOWTs are being developed, cost is a main barrier to commercializing the FOWT system. This article aims to use a shape parameterization technique within a multidisciplinary design analysis and optimization framework to alter the shape of the FOWT platform with the objective of reducing cost. This cost reduction is then implemented in 30 MW and 60 MW floating offshore wind farms (FOWFs) designed based on the static pitch angle constraints (5 degrees, 7 degrees and 10 degrees) used within the optimization framework to estimate the reduction in the levelized cost of energy (LCOE) in comparison to a FOWT platform without any shape alteration–OC3 spar platform design. Key findings in this work show that an optimal shape alteration of the platform design that satisfies the design requirements, objectives and constraints set within the optimization framework contributes to significantly reducing the CAPEX cost and the LCOE in the floating wind farms considered. This is due to the reduction in the required platform mass for hydrostatic stability when the static pitch angle is increased. The FOWF designed with a 10 degree static pitch angle constraint provided the lowest LCOE value, while the FOWF designed with a 5 degree static pitch angle constraint provided the largest LCOE value, barring the FOWT designed with the OC3 dimension, which is considered to have no inclination.

Keywords: FOWT; optimization algorithm; shape parameterization; CAPEX; fixed-bottom

Citation: Ojo, A.; Collu, M.; Coraddu, A. Preliminary Techno-Economic Study of Optimized Floating Offshore Wind Turbine Substructure. *Energies* **2024**, *17*, 4722. https://doi.org/10.3390/en17184722

Academic Editor: Frede Blaabjerg

Received: 23 June 2024
Revised: 5 September 2024
Accepted: 19 September 2024
Published: 22 September 2024

1. Introduction and Background

1.1. Background

Wildfires and excessive floodings have been seasonal climatic changes across the globe in the past decade. The need for clean energy to fight against the climate changes observed as a result of excessive greenhouse emissions over the years is driving the development of the offshore wind sector. This drive is pushing the exploitation of rich wind resources in deep waters with water depth greater than 60 m, requiring a deviation from the commercialized fixed-bottom foundation offshore wind technology. Resolving the issue of exploiting rich wind resources requires the use of floating foundation offshore wind technology that satisfies stability and durability requirements in any environmental conditions. With more than three-quarters of the world's offshore wind resource potential available in waters deeper than 60 m along the coastline of many countries, the potential for fixed-bottom offshore wind systems becomes limited [1]. This highlights the need for FOWT technology in order to see a true global growth in clean technology to contribute to the reduction in greenhouse emissions.

Mega-Watts' (MW) scale floating technologies have only been tested in the last ten years through demonstration and pilot projects in both Europe and Asia. With the completion of some demonstration projects, FOWT technology is currently in the pre-commercial phase, with a shift in emphasis moving towards larger power capacity turbine schemes [1].

It is anticipated that, by 2026, FOWT system deployment will move into the commercial phase, with yearly installations surpassing 1 GW–a milestone achieved by fixed offshore wind in 2010 [2].

The concept of the floating offshore wind turbine was conceived in the 1970s [3]. Despite its early conception, FOWT is still in the pre-commercial stage, leaving the fixed-bottom foundation/platform as the dominant technology in the OWT sector [4]. FOWT foundation technology complements its fixed-bottom foundation counterpart as it offers capabilities for setting up the FOWT system offshore in deep waters while ensuring less invasive actions on the seabed which potentially present a less expensive technology [5]. FOWT technology provides the capability to move further offshore to exploit better wind resources while also limiting visual impact from land and moving away from competing with other users of the sea [6]. Additionally, due to less-invasive construction methods on the seabed than fixed-bottom designs, floating foundations typically provide environmental advantages over them [7]. The world's forecast growth of floating offshore wind was 17MW in 2020 to 6.5 GW by 2030. A review of the forecast was conducted in 2021 with the forecast increased to 16.5 GW of floating offshore wind capacity by 2030 [1], highlighting a significant interest in increasing the capacity of FOWT technology in reducing greenhouse emissions. The floaters required for offshore wind must provide adequate buoyancy to support the weight of the wind turbines and also have the capability to constrain its motion within allowable limits [8].

Three main floating platform concepts (spar, semisubmersible and tension leg platform) from the oil and gas industry are the early adapters (early to market floaters) in the FOWT sector. The stabilization mechanisms of the three platforms highlighted are ballast, waterplane/buoyancy and mooring stabilization, respectively. As highlighted in Leimeister, et al. [9], several floating solutions have currently been developed that are anticipated to be appropriate and considerably financially viable in depths greater than 60 m. These new floating solutions still adapt the stability mechanisms used in the early-adapter floaters from the oil and gas sector.

The ballast-stabilized spar requires a large ballast that is deep at the bottom of the floater to move the center of gravity of the system below the center of buoyancy in order to provide a restoring moment or stabilizing righting moment which counteracts the inclining moments. In the waterplane area or buoyancy-stabilized semi-submersible, a large second moment of waterplane area with respect to the rotational axis creates the restoring moment to counteract against the rotational displacement.

The mooring-stabilized TLP utilizes high-tension mooring lines to generate the restoring moments to counteract the effect of any inclining moment on the structure. The choice of the platform used for a FOWT system will also depend on elements like water depth, localization potential, local infrastructure and various turbine designs. As a result, the market will likely adjust to changing situations rather than rationalize around a single sort of floating platform [1].

The average CAPEX of a floating platform is higher than that of a fixed-bottom platform. As highlighted in [10], the best rate value CAPEX for a fixed-bottom OWT is 2435 k€/MW while for spar, semi-sub and TLP FOWTs, the CAPEX are estimated at 3025 k€/MW, 3080 k€/MW and 2970 k€/MW, respectively. The floating substructure of a reference wind power plant accounts for approximately 29.5% of the CAPEX for the project, in contrast to 13.5% for a fixed-bottom reference project [11]. These average values can be significantly higher or lower depending on the floater type employed and will significantly impact the profitability of the project. It is expected to see innovation in design, construction, operation and maintenance as the industry evolves to facilitate the building and operation of larger FOWT projects. The construction of FOWT systems can be in ports or sheltered waters making use of specialized vessels. Major maintenance and repair activities might also be carried out away from the site using the innovative "tow-to-port" maintenance capability. Continuous innovation in design is expected to yield new technologies and products capable of supporting better mooring and anchor solutions,

deep water substations and dynamic cabling, management of FOWT system's response to environmental conditions and sea-states and the design of floating platforms.

Bringing the cost of floaters/platforms used in the FOWT system down to the level of fixed-bottom platforms needs extensive developmental process and ideas exploration. Some of the processes and ideas that can be explored in driving down the cost of FOWT systems are:

1. Geometric shape parametric design, analysis and optimization of the FOWT platform [12–15];
2. Upscaling design platform to fit with larger turbines [16–18];
3. Multidisciplinary design analysis and optimization of all components within the FOWT system (Turbine, tower, platforms, mooring lines and anchors) [19–21];
4. Provision of government subsidy to floating wind projects in the precommercial stage to add economic value until the FOWT technology becomes cost-competitive with the fixed-bottom OWTs [22].

Currently, most floaters in offshore wind are modeled after the conventional oil and gas stability mechanism of ballast–spar, waterplane area–semi-submersible and mooring–Tension Leg Platform. This work is addressing a gap of platform shape alteration using the spar as a case study and assessing the economic impact of the optimized shape in a FOWF. This study has the potential to identify optimal novel design shapes within a large design space in a reduced computational time before detailed hydrodynamic response analyses are conducted with time domain tools.

1.2. B-Spline Curve

The uniqueness of this study lies in the use of a B-spline polynomial curve to model a spar platform within an optimization framework. The use of B-spline has been extensively used in other sectors like the automobile and oil and gas [23,24]. B-spline's notable use in modeling within the FOWT sector is seen in the work of [25] where it was used in describing the circumferential T-ring stiffeners within the hull of spar platform to reduce the number of design variables and corresponding computational time.

The novelty of using the B-spline technique to model a FOWT platform lies in its capacity to provide a highly flexible and smooth representation of complex geometric shapes. B-splines offer a parametric approach that allows for precise control over the shape of the model, enabling designers to efficiently explore and optimize various design configurations within the specified design space.

This work is exploring the use of B-spline to model a spar FOWT platform within an optimization due to some of its unique properties detailed in [23] and highlighted below.

- A B-spline curve has local propagation properties which make it possible to locally alter the shape of the design rather than altering the global shape as is the case with most modeling curves like the Bezier curve. A given control point influences 1 or 2 or n curve segments. This ensures B-spline localized shape control. This property is important as it gives the designer the capability to alter different segments of the design, including altering the shape geometry as shown in Section 3.2;
- The number of segments in a B-spline curve is derived from the degree and the number of control points in the curve, i.e., the number of segments is $n - k + 2$ where n is the number of control points and k is the degree/order of the curve;
- The continuity of a B-spline curve can go beyond the C2/curvature continuity to ensure a higher level of smoothness of the curve. A B-spline curve is $C^{(k-2)}$ continuous;
- A B-spline curve is invariant under affine transformation;
- A B-spline curve has partition of unity properties.

B-spline is an essential design approach within this framework as it allows designers to modify the positions of control points to deform the shape of the B-spline curve or surface, enabling the exploration of different design variations while maintaining smoothness and continuity. This level of adaptability and control can be potentially advantageous in

the dynamic and challenging environment of FOWT platforms, where intricate shapes and structural considerations are crucial. The B-spline technique's capability for thorough design space exploration and its ability to balance geometric complexity with manageability contributes to its novelty in enhancing the design, analysis and optimization processes for a spar FOWT platform in this study.

Details of the B-spline equation and the optimization problem of this study are presented in Section 3.2. The main aim of this study is to investigate the economic implications of use of the local propagation property of B-spline to alter the geometric shape of a spar FOWT within a design, analysis and optimization framework on a 30 MW FOWF and also the cumulative effect of this bespoke approach and economies of scale on a 60 MW FOWF.

1.3. FOWT Techno-Economic Feasibility-Overview

At the turn of the millennium, the total installed costs for offshore wind farms were initially evaluated based on the costs of existing shallow-water farms and extrapolated to deeper waters for deep-water offshore farms [26]. The extrapolation resulted in increased costs of foundations, grid connection and installation. The design approach for these new offshore wind farms resulted in a notable trend. It led to an increase in the average cost of offshore wind installations, which rose from 2300 €/kW in 2000 to a peak of 5000 €/kW during the period from 2011 to 2014. However, starting in 2015, there was a positive shift in this trend. The total costs of FOWFs began to decrease, ultimately reaching 4000 €/kW in 2018 [7,26,27].

The predicted cost for FOWFs is expected to decrease, according to recent studies, primarily due to technological advancements. These allow capacity factors to rise while lowering overall installation and maintenance costs [26]. Additionally, the rise in this technology's competitiveness can also be efficiently improved by the following:

- Aerodynamics, Hydrodynamics, Servodynamics, Elastodynamics (AHSE) optimization within a MDAO framework and adequate use of shape parameterization technique with an optimization algorithm to optimize platforms in accordance with specified design objectives and constraints;
- Platform upscaling techniques to bigger and heavier turbines;
- Increase in designers' experience, which reduces project development costs and risks;
- The increase in the industry maturity, bringing lower capital cost;
- Presence of economies of scale across the value chain.

The future development of floating wind technology will benefit from accurate financial analyses sustaining the economic and technical value of FOWTs. Some of the techno-economic study on FOWTs are detailed herein.

A shape parameterization study of the FOWT platform was conducted by [28] to alter the shape of a spar platform coupled to a 5 MW OC3 turbine, reducing the mass of the spar platform and leading to a reduction in the required cost of steel for manufacturing the spar platform. This study used a B-spline parameterization technique within a design analysis and optimization framework using a metaheuristic pattern search optimization algorithm to explore the design space and produce an optimal design. The optimal design in the study is a spar variant platform with altered shape and lower mass than the standard OC3 platform. The limitation in this study is that the cost of steel for the optimal spar was the only financial parameter to assess the economic feasibility of the FOWT system.

Ghigo et al. [29] conducted a study on platform optimization and cost analysis in a floating offshore wind farm. This study focused on the choice of a floating platform that minimizes the global weight, in order to reduce the material cost, while ensuring buoyancy and static stability. Subsequently, the optimized platform is used to define a wind farm located near the island of Pantelleria, Italy in order to meet the island's electricity needs. A sensitivity analysis to estimate the LCOE for different sites is presented, analyzing the parameters that influence it most, like Capacity Factor, Weighted Average Capital Cost (WACC) and number of wind turbines. The study concluded that the decrease in many

Capex cost items and the evolution of the offshore wind market will make this technology even more competitive in a few years.

Ioannou, Liang, Jalón and Brennan [11] conducted a preliminary parametric techno-economic study of offshore wind floater concepts. This study investigated through a parametric study the total mass and cost of three floater concepts: spar, barge and semi-submersible, particularly focusing on the material and manufacturing costs. A survey from floating offshore wind industry professionals was conducted to determine the manufacturing complexity factors' values, which were used to calculate the manufacturing cost. The main conclusion of this work is that, given the specified conditions, steel-based semi-sub structures proved to be the most expensive configuration followed by spar as spar prices fall with higher draught values due to the reduction in ballast mass. The barge solution is the least expensive option of the three configurations. Also, the study highlighted that the risks and benefits of different configurations should also be considered, as they could lead to savings throughout the service life of the asset.

Castro-Santos, et al. [30] presented an approach for evaluating the lifecycle costs of a combined or hybrid floating offshore renewable energy system like a FOWT. Their methodology expressly takes into account the life cycle stages, amongst which are concept generation and definition, design and development, manufacturing, installation, exploration, exploitation and decommissioning. It is a tool for strategic planning and decision-making, allowing for a better understanding of technical advancements and factors that could either expedite or slow down the growth of the FOWT sector. Their findings from two sites show that the exploitation, manufacturing and installation costs are the most important lifecycle costs on the LCOE, but the most important of the three costs could be site-dependent.

Martinez and Iglesias [31] conducted an extensive study that mapped the LCOE for floating offshore wind in the European Atlantic. They emphasized the importance of understanding LCOE spatial variations to identify suitable areas for the development of FOWT technology. The study focused on floating semi-submersible platforms, presenting a comprehensive LCOE mapping across the European Atlantic. Accurate energy production estimates were obtained by combining hindcast wind data and an exemplary wind turbine's power curve. The study revealed the lowest LCOE values (around 95 €/MWh) in wind-rich regions like Great Britain, Ireland, the North Sea and NW Spain. In contrast, higher LCOE values (approximately 125 €/MWh) were observed off Portugal and Norway, and significantly higher values exceeding 160 €/MWh were noted in the Gulf of Biscay and south of the Iberian Peninsula.

Filgueira-Vizoso et al. [32] evaluated the technical and economic viability of floating offshore wind platforms. Their work defined an economic assessment approach for TLP platform-based offshore wind farms. Life-cycle costs were categorized into stages including conception, design, manufacturing, installation, exploitation and dismantling. Economic indicators like IRR, NPV, DPBP and LCOE were assessed based on cashflow. The study focused on a TLP platform designed by CENTEC, considering an 880 MW farm located along the European Atlantic Coast in the northwest region of Galicia, Spain. Eighteen case scenarios were analyzed, with varying electric tariffs and capital costs. The study underscored the impact of electric tariffs on economic indicators. The optimal outcome emerged for a tariff of EUR 150/MWh and a 6% cost of capital, yielding an IRR of 18.34%, NPV of EUR 2636.45 million, and DPBP of 8 years. The farm's LCOE reached a minimum of EUR 54.33/MWh, rendering the platform economically feasible due to its IRR-surpassing capital costs.

Pham and Shin [33] introduced a novel conceptual design for a spar-type platform, intended to accommodate a 5 MW offshore wind turbine. This innovative concept effectively addresses challenges associated with the OC3-hywind model, notably the elevated nacelle acceleration and tower-base bending moment. This achievement is accomplished through the incorporation of an open moonpool positioned at the platform's center. By leveraging the water column within the moonpool, the mass and inertia of the entire wind system are augmented along the x and y axes. By appropriately sizing the moonpool

diameter, it becomes possible to mitigate nacelle acceleration and tower-base bending moment concerns.

Campos et al. [34] presented a novel approach to achieving a cost-efficient offshore wind turbine floating platform. This concept revolves around a monolithic floating spar buoy design. The innovation lies in the integration of both the tower and floater components as a seamless, continuous concrete structure. This concept promises significant cost savings, not only during the construction phase but also throughout the platform's operational lifespan. The inherent design translates to minimal maintenance requirements. Comprehensive insights into the construction and installation processes are provided in Campos, Molins, Gironella and Trubat [34], considering the distinctive demands of the monolithic design. The authors conducted a comparative analysis of costs between steel and equivalent concrete platform designs and their findings underscore a material cost reduction exceeding 60% for the concrete design, reinforcing its economic viability.

Lerch et al., 2018 [35], conducted a study exploring three platform concepts (spar, semi-submersible and TLP) for FOWTs, situated across different locations and comprising a 500 MW floating offshore wind farm. Their findings underscore the competitiveness of FOWTs, demonstrating their capacity to generate energy at an equivalent LCOE compared to fixed-bottom offshore wind technologies. They identified significant parameters influencing the LCOE of the FOWFs with potential for substantial cost reductions. Notably amongst these parameters are manufacturing-related costs, including those of the wind turbine, substructure and mooring system. These parameters are key factors driving LCOE variations across all concepts and offshore sites. They also highlighted how innovative ideas such as dedicated construction and assembly facilities tailored for floating wind can further contribute to cost reduction, particularly during the manufacturing phase of FOWF components.

Castro-Santos et al. [36] developed a method to assess the economic viability of deep-water offshore wind farms by considering their economic factors. This procedure involves the use of various economic parameters, including internal rate of return, net present value and levelized cost of energy. Notably, the research indicated that among the considered platform types, the semisubmersible platform exhibited the most favorable levelized cost of energy (LCOE) value, followed by the spar platform and the TLP platform.

1.4. Optimization Review

Some innovative studies to improve the design and optimization of floaters also contribute to the process of maturing FOWT technology and making it as economically competitive as its fixed-bottom foundation counterpart. Some of the innovative technical and optimization studies are highlighted herein: -

Hall et al. [37] focused on optimizing the hull shape and mooring lines of FOWTs across various substructure categories. This optimization was carried out using a Genetic Algorithm (GA) and a frequency domain model based on OpenFAST-3.3.0 software. Their model is a linear representation of hydrodynamic viscous damping and did not include a representation of wind turbine control. The GA was employed for both single and multi-objective optimization. The study's outcomes revealed an unconventional design, highlighting the need for further refinement of cost functions in the optimization process.

Karimi et al. [20] enhanced the research conducted by Hall et al. [37] by implementing a new optimization algorithm and a linearized dynamic model, leading to improved optimal solutions. In their study, Karimi et al. [20] introduced a fully coupled frequency domain dynamic model and a design parameterization approach. This allowed for the evaluation of system motions and forces in scenarios involving turbulent winds and irregular waves. Furthermore, they employed the Kriging–Bat optimization algorithm, a surrogate-based evolutionary approach, to facilitate the exploration and exploitation of optimal designs across three stability classes of platforms: MIT/NREL TLP, OC3-Hywind Spar and OC4-DeepCwind semi-submersible platforms. This optimization primarily aimed to assess the cost implications of platform stability, as reflected by the nacelle acceleration objective

function, across these three categories of FOWT platform stability. This study shows an enhanced correlation between cost and substructure design compared to the previous work by Hall et al. [37].

Hegseth et al. [25] conducted a comprehensive design optimization for an integrated system including the platform, tower, mooring system and blade pitch controller for a 10 MW spar-type floating wind turbine. The study involved optimizing various design parameters for the spar, including its diameter and wall thickness along ten distinct sections. The hull of the spar is equipped with circumferential T-ring stiffeners, which reduced the required computational effort by ensuring the number of design variables is decreased by introducing B-splines with four control points for the ring stiffener parameters. The study's findings revealed that the optimized platform exhibits a relatively small diameter within the wave zone and assumes an hourglass shape beneath the waterline. This particular design serves to minimize wave-induced loads on the structure. Additionally, the distinctive shape enhances the system's restoring moment and natural frequency in pitch, resulting in an enhanced dynamic response within the low-frequency spectrum.

Dou et al. [38] introduced an optimization framework tailored for the support structure of floating wind turbines, specifically the spar-buoy floater, which also includes the mooring system. This framework was developed from frequency domain modelling, and it extends its analytical capabilities to provide design sensitivities for various design criteria. This unique capability facilitates rapid optimization by leveraging on the Sequential Quadratic Programming (SQP) optimization algorithm.

The optimization techniques discussed in Hall et al. [20], Hegseth et al. [25], Hall et al. [37] and Dou et al. [38] also reviewed above have the capability of reducing the computational time for the design and analysis of FOWTs. The reduction in time to search a large design space and identify optimal solutions allows stakeholders to make informed decisions that can potentially help in driving down the cost of FOWTs to the levels of cost in fixed-bottom foundation turbines.

This study aims to further reduce computational time for design of bespoke FOWTs and also reduce the LCOE of a FOWF by integrating shape parameterization techniques using a B-spline parametric curve to model a spar. The design and analysis process of the spar is integrated with a gradient-free optimizer to search the design and analysis space and identify the optimal design within a minimal amount of design and analysis time.

1.5. Financial Parameters

Some financial parameters employed to assess offshore wind projects encompass the NPV, IRR, DPBP and LCOE, among others [30,32,39]. These metrics play a pivotal role in evaluating the project's profitability and its appeal to stakeholders. For this study, the primary focus is on the LCOE.

LCOE

The LCOE is theoretically the price at which electricity would have to be sold to reach the break-even point. It is therefore a fundamental parameter in analyzing the economic viability of an energy project and serves as a standardized approach to comparing costs of different energy sources [31]—onshore/offshore wind, solar, coal and hydro. The LCOE can be defined as the ratio of the costs of an energy project to the electricity production over its lifetime, which is usually expressed as highlighted in Equation (1):

$$\mathrm{LCOE} = \frac{\sum_{t=1}^{n} (\mathrm{CAPEX_t} + \mathrm{OPEX_t})(1+\mathrm{r})^{-t}}{\sum_{t=1}^{n} (\mathrm{AEP_t})(1+\mathrm{r})^{-t}} \quad (1)$$

where the costs are subdivided into CAPEX, i.e., the costs spent prior to the operation of the project, and OPEX, i.e., the costs of the electricity production and maintenance of the energy farm. AEP represents the annual energy production of the project, which constitutes the main source of income. The variable t represents the lifetime of the project in years and *r* denotes the discount rate.

While this study focuses on platform design to influence the CAPEX reduction and subsequently the LCOE, other parameters like the OPEX and AEP are essential in determining the LCOE. The AEP is an important factor in determining the LCOE and it is a function of wind resources; hence, understanding how wind patterns are formed over several kilometers is essential. The mesoscale impact of the sea surface on offshore wind farms is a complex interplay of atmospheric and oceanographic factors that can significantly influence wind patterns and, consequently, the performance of the wind farm. Understanding these impacts is crucial for optimizing the design, placement and operation of turbines to maximize energy production and ensure the structural integrity of the wind farm over its operational life.

Mesoscale impact of the sea surface on the performance of offshore wind farms is well detailed in [40]. The study explored the impact of ocean-atmosphere interactions on offshore wind farm performance by coupling the Weather Research and Forecasting (WRF) model with a sea surface model and refined wind farm parameterization. The findings reveal that ocean interactions significantly affect wind farm wakes and power output, with notable momentum and wind speed deficits spreading horizontally across the sea surface. The wake from offshore turbines mixes more readily and extends less than on flat land, causing a 10% reduction in power output for downwind turbines. Additionally, increased wind shear from ocean waves decreases power output by about 3.5%. This highlights the importance of using coupled air–sea-wind farm models for accurate offshore wind farm performance assessment. Understanding the impact of ocean interactions also helps in informing the spacing between offshore turbines to enhance dynamic wake modulation and wake recovery.

1.6. Creativity and Structure of the Study

The creativity of this work lies in its capability to provide feasible designs with unique shapes that satisfy the fundamental design requirement of a FOWT system, which is stability (hydrostatic and dynamic, considering the effect of waves and wind). Take the Spar-buoy as a case study as shown in Figure 1. The traditional Spar-buoy design is a straight cylinder at the base with a transition piece at the waterline to the tower base. The automated altered geometric shape to be further discussed in this study has different diameters at varying control points along the length of the spar. This diameter-varying capability allows for shape alteration and steel mass reduction in the spar. While this study has been limited to the ballast-stabilized Spar-buoy, the creativity of this concept can be extended to the waterplane-stabilized Semi-submersible and the mooring-stabilized TLP.

Figure 1. Traditional spar model vs shape parameterized spar concept.

This investigation will be conducted with the use of the LCOE financial parameter highlighted in Section LCOE in conjunction with the methodology discussed in Section 2. The techno-economic study highlighting the impact on costing is detailed in Section 3 and adequate conclusions presented in Section 4.

2. Methodology

2.1. Overview

The majority of wind turbines are rated according to their power output [41], and each rated turbine has a unique rotor nacelle assembly design. Effecting quick optimization changes on the FOWT system for economic feasibility purposes is best performed on the substructures platform, mooring and anchor designs. As highlighted in Section 1, the cost of a FOWT platform is substantially more than that of a fixed-bottom design configuration. It has been shown that the mass of steel used in the design of ship hull and FOWT platforms can be reduced [13,28], respectively, using shape parameterization techniques like NURBS and B-spline within an optimization framework. This reduction in the mass of steel material used in manufacturing the hull/platform substantially reduces the cost of the structure. For mooring optimization, Munir et al. [42] showed that FOWTs with shared mooring systems can be one of the most cost-effective solutions in reducing mooring costs and also mooring footprint on the seabed.

The methodological approach selected in this study is to estimate the LCOE of 30 MW and 60 MW wind farms using an optimized platform distinguished by applying static pitch angle constraints in the optimization process. The optimal platforms based on the constraints are utilized in hypothetical wind farms to compare economic feasibility using the LCOE financial parameter. The process adopted is similar to the approach used in [28] with an additional task of preliminary LCOE estimation added to the framework. The proposed methodology for the exploration, exploitation and preliminary LCOE estimation of a FOWT farm is to firstly define a parameterization scheme with a robust design space configuration using the B-spline/NURBS parameterization technique. This is followed by assessing the design models within the design space with frequency domain analysis tool Sesam suite by DNV (Genie and HydroD/Wadam). The next stage is to integrate the analysis with the optimizer for optimal design selection for the 5 degree, 7 degree and 10 degree static pitch angle. The last stage involves estimating the LCOE for a 30 MW and a scaled up 60 MW FOWFs—for each optimal design selected for the FOWFs—30 MW and 60 MW. For this preliminary assessment, the hydrostatic analysis is sufficient to estimate the mass of the optimal platform. The described methodological process is shown in Figure 2. The schematic configuration of the FOWF estimated is shown in Figure 3.

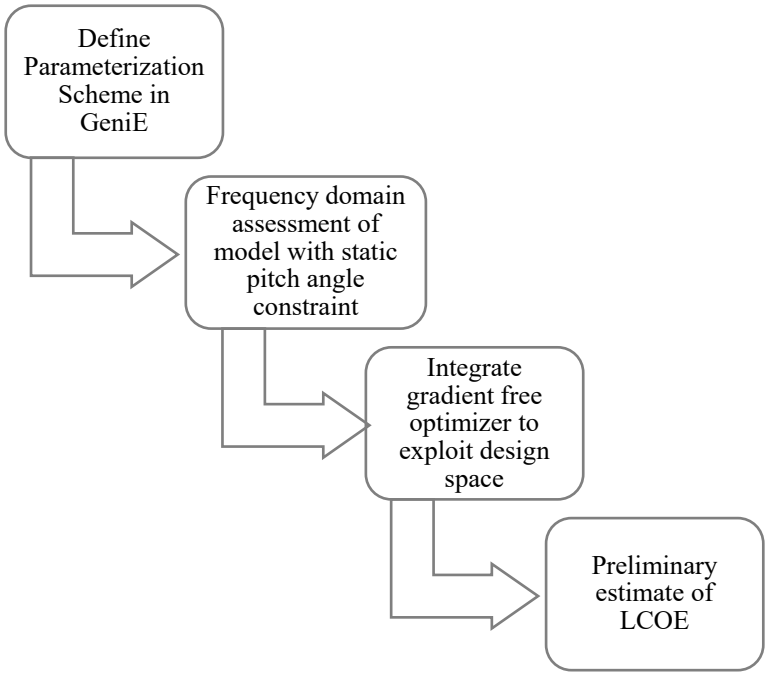

Figure 2. Platform shape optimization and LCOE estimation of a FOWF.

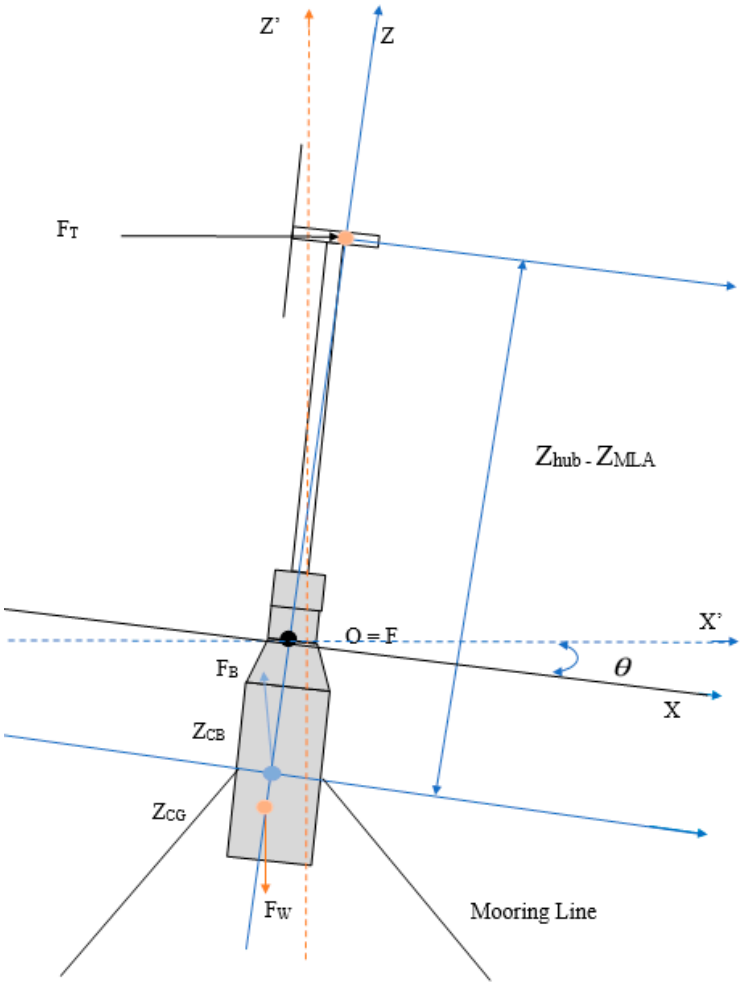

Figure 3. Sketch of forces and reference points of a representative spar FOWT.

2.2. Hydrostatics and Stability

The design and optimization of any type of floating offshore wind system must satisfy the stability requirement. This needs a detailed hydrostatic assessment to ensure the floater provides enough buoyancy to support the turbine, tower and mooring lines while also restraining the heave, roll and pitch motions within allowable limits. The hydrostatic equations in pitch for the available stability mechanisms based on ballast, waterplane area and mooring systems are represented with the buoyancy equations and the restoring equation highlighted in Equations (2) and (3), respectively:

$$M_{Total} = \rho_w V \tag{2}$$

$$(\rho_w g I_y + F_b z_{CB} - F_w z_{CG} + C_{55,moor})\theta = F_T(z_{hub} - z_{MLA}) \tag{3}$$

where M_{Total} is the total mass of the FOWT system, which consists of the substructure components (platform, mooring lines, ballast and anchors) and the superstructure components (tower and turbine), ρ_w is the water density and V is the volume of the displaced fluid, g is the acceleration due to gravity, I_y is the second moment of area of the initial waterplane area (within the approximation of small angle of inclination, the waterplane area remains constant) with regard to the X axis, F_b is the buoyancy force, Z_{CB} is the center of buoyancy (the point at which the resultant buoyancy forces on the body acts), F_w is the system's weight force, z_{CG} is the system's center of gravity (the point at which the total systems weight $C_{55,moor}$ is the contribution of the mooring stiffness to the pitch stiffness), θ is the pitch inclination angle, F_T is the thrust force from the wind speed and z_{hub} is the hub

height. The expressions on the left-hand side of Equation (3) highlight the stability mechanisms within the FOWT system. The first expressions highlight the water plane stability mechanism, the second and third expressions represent the ballast stability mechanism [11], and the fourth expression represents the mooring stability mechanism [43]. A schematic highlighting all the forces and reference points mentioned for a representative spar FOWT system is shown in Figure 3.

2.3. Floatability and Maximum Inclination Angle Requirements

The floatability requirement is satisfied with Equation (2), which highlights the equality of the buoyancy force of the platform and the total mass of the substructure. With regard to the maximum angle of inclination, it is equivalent to imposing a minimum pitch stiffness derived from Equation (3) and highlighted in Equation (4) [11]:

$$\frac{F_T(z_{hub} - z_{MLA})}{(\rho_w g I_y + F_b z_{CB} - F_w z_{CG} + C_{55,moor})} \leq \theta_{max} \quad (4)$$

where $(\rho_w g I_y + F_b z_{CB} - F_w z_{CG} + C_{55,moor})$ is the minimum total stiffness resulting in the maximum angle of inclination.

The expression in Equation (4) is very important in the early stages of design as a constraint for exploring the design space based on the allowable static pitch angle required for the FOWT system prior to conducting detailed analysis on the design.

3. Results and Discussion—Techno-Economic Analysis

3.1. Overview

As highlighted in Section 1.5, the LCOE is an essential financial parameter for assessing any energy-generating project, including wind farms, as it is the ratio of the costs of an energy project to the electricity production over its lifetime. A host of factors can reduce the LCOE, several of which are listed below and detailed in Markus Lerch [22].

- CAPEX reduction due to optimization
- Cost reduction potential through industrialization
- Cost reduction due to economies of scale
- Cost reduction due to discount rate.

Exploring the four factors listed above, coupled with other factors like improving permitting of FOWFs, improved supply chain and government subsidies have the potential to increase the commercial viability of the FOWT concept and bring the LCOE cost for FOWT concepts down to what is standard for fixed-bottom offshore wind turbines. For the purposes of this study, the preliminary techno-economic assessment is based on the CAPEX reduction due to optimization. The CAPEX cost this study influences is the cost of the platform, which makes up about 30% of the total CAPEX cost of a floating wind project [44]. The shape of the platform is geometrically optimized with the objective of reducing the mass of steel used, which invariably should reduce the cost of steel. The technical details required for shape optimization are highlighted in Section 3.2. The effect of mass reduction in steel on platform development is highlighted in Section 3.3.

3.2. Technical Assessment

A high-level numerical simulation from a reference FOWT model (NREL OC3 spar platform) is assessed within a multidisciplinary design analysis and optimization framework to explore, exploit and select optimal design variants from the design space. The optimal design variants are then assessed with a preliminary economic feasibility study using a representative wind farm with material and cost assumptions from the literature.

3.2.1. Reference Design

The reference design for this study is the OC3 spar platform supporting a conventional three-bladed, upwind variable-speed 5 MW baseline horizontal axis wind turbine.

The geometric and structural properties of the OC3 spar platform are highlighted in Tables 1 and 2, respectively.

Table 1. Geometric parameters for OC3 Spar [45].

Parameters	Dimensions (m)
Top cylinder diameter	6.5
Height of top cylinder	4
Diameter at top of transition area	6.5
Diameter at base of transition area	9.4
Height of transition area	8
Bottom cylinder diameter	9.4
Bottom cylinder height	108
Distance of platform keel to still water level (Draft)	120

Table 2. Floating platform structural properties [45].

Parameters	Values per Literature
Platform mass (including ballast)–(kg)	7,466,330
Center of mass below Sea water level (SWL)–(m)	89.9155
Platform roll inertia- about centre of mass–kgm^2	4,229,230,000
Platform pitch inertia- about centre of mass–kgm^2	4,229,230,000
Platform yaw inertia- about central axis–kgm^2	164,230,000

3.2.2. Technical Selection of Optimal Variants within a Design Analysis and Optimization Framework

This study assesses a high-level model design, hydrostatic analysis and optimization study of a spar substructure discipline in a FOWT system. The design is conducted using a B-spline shape parameterization technique to enable the exploration of a rich design space for optimal variant selection. B-spline is utilized due to its capability to alter the shape of the design locally when the control point values are changed. This gives the designer an effective control over the shape with the capability of exploring a richer design space. A metaheuristic pattern search optimization algorithm is used to select the optimal design satisfying the specified objective function and constraints provided within the optimization framework. The specified objective function in this study is minimizing the mass of the platform. This objective is estimated by conducting a hydrostatic analysis using DNV suite–GeniE-8.4-06 and WADAM-10.1-03 stability software. The process involved in the technical selection within the optimization framework is detailed herein:

B-Spline Design of Spar

A B-spline approximation is a specific instance of the Bezier curve, frequently employed in engineering to afford designers greater control when modifying the curve [23,46]. B-spline is a blended piecewise polynomial curve that closely passes through a set of control points. It is termed "piecewise" because the blending functions utilized to combine the polynomial curves can vary across different segments of the curve. Consequently, when a control point is altered, only the segment of the curve defined by the new point and its adjacent vertices undergoes modification, rather than the entire curve. This makes it suitable for shape variation, as intended in this study.

The B-spline parameterization technique is selected for this study due to its many suitable properties, which include its local propagation property for effective control of shape of a design, its capability to explore large and rich design space, its invariance property under affine transformation and its quick simulation turnaround time.

Samareh [47] showed that several low-degree Bezier segments can be used to represent a complex curve rather than using a high-degree Bezier curve. The resulting composite

curve from this low-degree representation is a spline more accurately referred to as B-spline. A multisegmented B-spline is described in Equation (5) [47].

$$\overline{\mathrm{R}}_{(\mathrm{U})} = \sum_{\mathrm{i}=1}^{\mathrm{n}} \overline{\mathrm{P}}_{\mathrm{i}} \mathrm{N}_{\mathrm{i,p}}(\mathrm{u}) \tag{5}$$

where $\overline{P}_i$ are the B-spline control points, p is the order/degree, $N_{i,p}(u)$ is the I th B-spline basis function of degree p. B-spline form can represent complex curves more efficiently and accurately than other curve representation like the Bezier, cubic Hermite spline, cubic spline and polycurves.

This multi-segmented curve in Equation (5) is used in modelling the curve-defining surface of the spar platform used for the hydrostatic analysis of the FOWT system's substructure. Modelling was conducted with the B-spline tool in DNV Sesam GeniE software.

Hydrostatics and Optimization

The high-level hydrostatic and optimization assessment in this study is conducted synchronously to obtain the optimal design. The hydrostatic assessment is based on the stability Equations (2) and (3) highlighted in Section 2, in which the buoyancy force of the spar from the volume of liquid it displaces is equivalent to the total mass of the system, while also considering the contribution of the stability mechanisms. Equation (3) is also evolved into Equation (4), which is an assessment of the maximum static pitch angle of the system. This is an important parameter which is used as a constraint in the optimization assessment of the optimal design variant.

The optimization algorithm used in this study is the pattern search method. Pattern search is a relatively inexpensive but rather effective optimization technique [48]. It is based on the heuristic of repeating the best search direction in exploratory moves as long as the response function improves. It also has the capability to be adequately dispersed among an appropriate number of starting points, granting it a multi-start ability to overcome noise and the danger of becoming trapped in local optima.

The optimization problem for this study is represented by Equation (6):

$$\begin{aligned} &\min_{x \in \mathbb{R}} J(x) \\ &subject\ to \begin{cases} xlower \leq x \leq xupper \\ h_i(x) = 0; i = 1\ to\ m \\ g_j(x) \leq 0; j = 1\ to\ p \end{cases} \end{aligned} \tag{6}$$

where x is a k-dimensional vector of design variables with lower and upper bounds, $J(x)$ is a single objective function, m is the number of equality constraints and p is the number of inequality constraints. The main objective for this optimization study is to minimize the mass of steel and, invariantly, the cost of the steel material used for the spar platform. The two main constraints considered within the optimization problem are as follows: three maximum static pitch angles of inclination of the system set at 5 degrees, 7 degrees and 10 degrees, respectively, and a positive ballast mass to ensure the floatability requirement.

Definition of the Optimization Problem

The parameters within the optimization problem are defined for a systemic and comprehensive examination of the system to improve its performance and meet the desired objective target for the design. The formal definition of the parameters within the optimization problem in Equation (6) are represented under the categories of design variables, objective function and constraint as detailed in the subsections below.

Design Variables

The design variable represents the radii of the spar at the control point, which the designers use effectively to alter the shape along the B-spline curve used in modeling

the wet geometry panel and the ballast compartment. The variables and description are highlighted in Table 3.

Table 3. Definition of design variables.

Platform Design Variables	Description	Compartment Design Variables	Description
x_1	Radius at tower base	-	-
x_2	Radius at MSL	x'_1	Radius at MSL
x_3	Radius at 4 m below MSL	x'_2	Radius at 4 m below MSL
x_4	Radius at 12 m below MSL	x'_3	Radius at 12 m below MSL
x_5	Radius at 30 m below MSL	x'_4	Radius at 30 m below MSL
x_6	Radius at 40 m below MSL	x'_5	Radius at 40 m below MSL
x_7	Radius at 50 m below MSL	x'_6	Radius at 50 m below MSL
x_8	Radius at 60 m below MSL	x'_7	Radius at 60 m below MSL
x_9	Radius at 70 m below MSL	x'_8	Radius at 70 m below MSL
x_{10}	Radius at 80 m below MSL	x'_9	Radius at 80 m below MSL
x_{11}	Radius at 90 m below MSL	x'_{10}	Radius at 90 m below MSL
x_{12}	Radius at 100 m below MSL	x'_{11}	Radius at 100 m below MSL
x_{13}	Radius at 110 m below MSL	x'_{12}	Radius at 110 m below MSL
x_{14}	Radius at 120 m below MSL	x'_{13}	Radius at 120 m below MSL

Objective Function

The objective function $J(x)$ in the optimization problem has the singular objective of measuring the minimum steel mass required for the platform designs within the design space. It is the structural mass of the geometrically modified spar, and the output is dependent on the hydrostatic assessment of the design models. For the optimization framework utilized in this study, a multi-start approach is employed to eliminate local minima issues; hence, the minimum of the minimum objective is selected as the optimal design variable in the explored design space.

Constraints

The constraints set in this optimization problem are the static pitch angle and the ballast mass. The static pitch angle calculated for the design is as highlighted in Equation (4). Three maximum static pitch angles of 5°, 7° and 10° are assessed in this study. A description of the constraints used for this optimization process is detailed Table 4.

Table 4. Optimization Constraints.

Inequality Constraint	Formal Expression	Description
g_{SP_05}	$g_{SP\_05} \leq 5^{\circ}$	Maximum static pitch less than or equal to 5°
g_{SP_07}	$5^{\circ} \leq g_{SP\_07} \leq 7^{\circ}$	Maximum static pitch greater than 5° and less than of equal to 7°
g_{SP_10}	$7^{\circ} \leq g_{SP\_10} \leq 10^{\circ}$	Maximum static pitch greater than 7° and less than of equal to 10°
$g_{ballast}$	$g_{ballast} \in \mathbb{R}$	Calculated ballast a positive real number

Optimal Selection

The control points on the B-spline curve in Sesam GeniE are interfaced with the optimization algorithm with Python codes to ensure that design variables within the specified boundary conditions in the optimizer are passed into Sesam Genie Java Script

without human intervention. This ensures the static pitch angle constraint highlighted in Equation (4) is coded into the optimization framework to integrate the hydrostatic analysis and the optimization algorithm for feasible optimal design selection.

The optimal design variables obtained for the 12-segmented spar with 13 control points and a modeled OC3 spar with its dimensions from the literature are highlighted in Table 5. The optimal variants in Table 5 based on the static pitch constraints of 5°, 7° and 10° are named case A, case B and case C, respectively. The model visuals from Sesam GeniE are presented in Figure 3, showing the wet surface geometry model for hydrostatic pressure integration and the corresponding compartment model for the ballast housing in the OC3 model and the corresponding three optimal cases. It can be seen that the each of the three optimized spars shows distinct geometric changes in comparison to the OC3 spar.

Table 5. Design data for selected models and OC3 spar.

OC3	Height	10	0	−4	−12	−30	−40	−50	−60	−70	−80	−90	−100	−110	−120
(m)	Radius	3.25	3.25	3.25	4.7	4.7	4.7	4.7	4.7	4.7	4.7	4.7	4.7	4.7	4.7
Case	Height	10	0	−4	−12	−30	−40	−50	−60	−70	−80	−90	−100	−110	−120
A (m)	Radius	3.25	6.91	6.86	7.22	6.04	5.00	0.55	0.50	0.50	0.50	0.50	0.53	3.38	3.92
Case	Height	10	0	−4	−12	−30	−40	−50	−60	−70	−80	−90	−100	−110	−120
B (m)	Radius	3.25	4.13	4.92	4.69	4.42	4.18	3.95	3.48	0.72	0.50	0.50	0.50	4.05	4.18
Case	Height	10	0	−4	−12	−30	−40	−50	−60	−70	−80	−90	−100	−110	−120
C (m)	Radius	3.25	3.72	4.13	4.01	3.89	3.77	3.65	3.54	2.64	0.50	0.50	0.50	3.65	3.71

For each case in Figure 4, the models are constructed using B-Spline curves, and a material density of 7850 kg/m^3 (steel) is used. A wall thickness of 0.0418 m is determined by utilizing the ratio of steel mass to buoyancy mass of 0.13, as highlighted in [49,50]. This wall thickness is selected based on the buoyancy mass of the NREL OC3 platform as a target value. Once the model is completed, Sesam GeniE is utilized to generate finite element mesh (FEM) files to be used for their hydrostatic assessment. Three FEMs generated for the hydrostatic assessment are the panel model FEM, the compartment model FEM and the total mass FEM. The ballast (seawater) goes into the compartment model, which adopts the outer panel/wet surface shape. A numerical code is developed determine the equivalent ballast required for the system's stability. The numerical code augments the total mass with the required amount of ballast to ensure the total mass is equal to the buoyancy mass.

Hydrodynamic analyses for the four cases were carried out using the Wave Analysis by Diffraction and Morison theory (Wadam) tool within the HydroD-4.10-01 software of the DNV Sesam suite. The total mass of the system (including the wind turbine, support platform and ballast) and the system's center of gravity are determined through Wadam analysis.

Optimal Variants and Hydrodynamic Response

This section focuses on the inherent design characteristics of the model, specifically the system's responses. These responses were assessed with WADAM within DNV Sesam HydroD software. The assessment was conducted in a wave height of 2 m (1 m wave amplitude) and a time period of 5 s to 200 s in steps of 1 s. These responses are evaluated for all three cases and are compared to the OC3 NREL 5MW FOWT system. Figure 5 shows the Response Amplitude Operators (RAOs) in surge, heave, pitch and horizontal nacelle displacement motion for the three design variant cases and the OC3 spar-buoy. The RAOs in Figure 5 show the frequencies of the peak motion response of the system. This is a very important tool for subsequent design of the system in different environmental conditions to ensure the system's responses avoid these peak motion response frequencies.

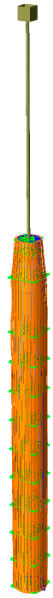

OC3 model hydrostatic wet geometry with B-Spline control points.

OC3 model transparent ballast compartment model within the Spar

OC3 Spar

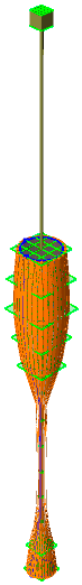

A. 5° static pitch hydrostatic wet geometry with B-Spline control points.

A′. 5° static pitch transparent ballast compartment model within the Spar

Case A

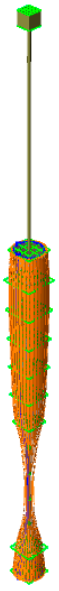

B. 7° static pitch hydrostatic wet geometry with B-Spline control points.

B′. 7° static pitch transparent ballast compartment model within the Spar

Case B

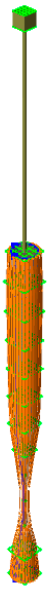

C. 10° static pitch hydrostatic wet geometry with B-Spline control points.

C′. 10° static pitch transparent ballast compartment model within the Spar

Case C

Figure 4. Optimal models from pattern search optimization algorithm and OC3 spar with corresponding compartment housing for ballast.

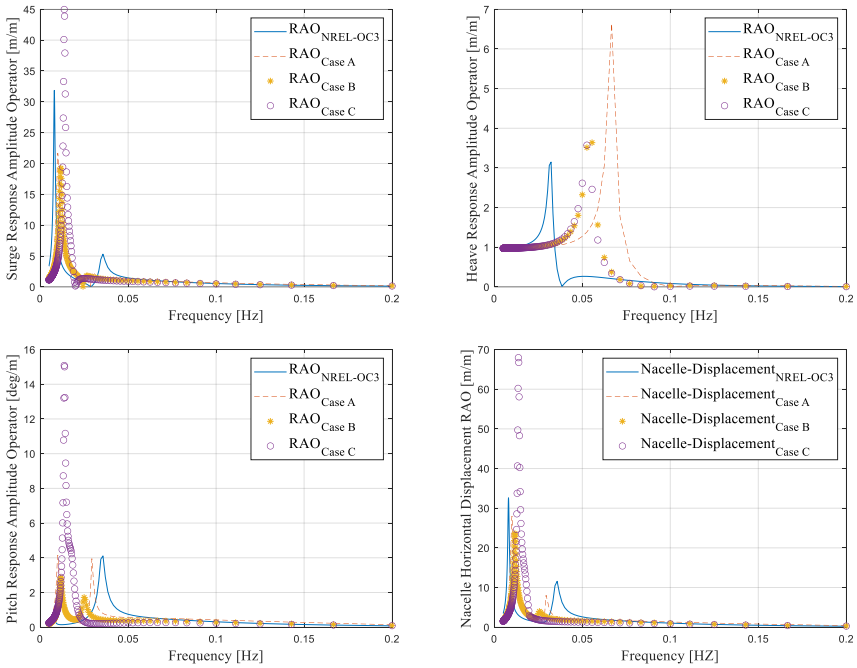

Figure 5. Surge, heave, pitch and nacelle displacement RAO.

From an operational perspective, case C is projected to display the highest motion across all considered degrees of freedom (DOFs), except for the heave DOF, where case A exhibits the greatest motion. In addition, the peak frequencies of the platform variants are all outside the first order wave excitation frequency range of 0.05 Hz to 0.2 Hz (5–25 s) in the surge, pitch and nacelle displacement responses. However, all the variants' peak periods are slightly within the first order wave excitation frequency range in the heave degree of freedom. This observation necessitates structural assessment for future work. While increasing the static pitch angle can potentially reduce the steel material used for manufacturing, it can have consequences for the fatigue loads in the tower as detailed in [51]. The authors conducted fatigue assessment on three 20 MW spar FOWTs with static pitch angles of 6°, 8° and 10°. They concluded that for a 20 MW FOWT, the largest fatigue damage at the still waterline was observed on the platform with a 10° static pitch angle. However, for the tower, the design with the 6° static pitch angle resulted in increased fatigue damage. In addition to the need for structural assessment, manufacturing can also be a challenge. However, technologies like Metal 3D printing and concrete slip-forming can potentially resolve manufacturing issues of the bespoke shaped spar.

3.3. Economic Feasibility Study

Some of the financial parameters used in assessing various projects in the literature are listed in Section 2. However, for the purpose of this study, the financial parameter chosen to assess the economic feasibility of the project to assess in this study is the LCOE.

The wind farm site used to assess the LCOE for this study is the Hywind wind park with a hypothetical water depth of 320m. It is essential to utilize measured data for the annual energy production (AEP) estimation of the project site. For this article, the AEP estimate of the Hywind site is taken from [52], where they have used the conventional Weibull distribution-based calculation for the estimated energy generation at the site during a studied climate period between 1991 and 2020. Their calculations are summarized as a fitting of the shape parameter 'k' and scale parameter 'c' related to the Weibull distribution to match the 30-year wind speed data, and a latter implementation of the power curve of the FOWT on the fitted histogram to estimate its energy production. Based on the work conducted in [52], the AEP value for the study is 139.8 GWh. Based on the AEP value of 23.2 GWh for a FOWT, the capacity factor worked out from a name-plate wind farm

of 30 MW is 52.97%. The capacity factor of 52.97% estimated from this study is much more conservative than the AEP capacity factor of 65% recorded for the HyWind Scotland floating wind farm site in [53].

3.3.1. CAPEX OPEX and DECEX Estimation

Due to the large number of cost components and frequent difficulty and complexity of the FOWT system, the Capital Expenditure (CAPEX) for a floating offshore wind farm (FOWF) is challenging to quantify. According to studies performed like the Carbon Trust in 2015 [54] and projects completed and some currently under construction like HyWind Scotland, Kincardine Offshore wind farm, Windfloat Atlantic and HyWind Tampen, the main cost items are related to turbines, towers, platforms, moorings, anchors and the balance of the system, amongst which are the cost of installation of the components that makes up the holistic system, cost of the electrical grid and connections to shore.

As highlighted in [55], CAPEX contributions are mostly determined analytically and/or as a function of the wind farm's installed power. The costs for components and installations are taken into account separately, in part because the former is moderately dependent on the site of installation while the latter heavily depends on the site of installation. The CAPEX is the largest cost, and it includes all investment costs to be faced before the commercial operation date [26]. The contributions to OPEX are also calculated analytically and/or as a function of the installed power of the wind farm, while contributions to DECEX (decommissioning and clearance) are calculated as a percentage of the installation procedure cost [55]. For this study, the CAPEX costs are going to be taken from the literature, and in cases where they are not available, assumptions are made. The percentage split of a spar FOWF's CAPEX, OPEX and DECEX for this study is 77%, 19% and 4% respectively as specified for a spar FOWF in [55].

The masses of the spar platform and corresponding estimated costs based on the platform's masses are shown in Table 6. The mass of the optimal design variant tends to reduce as the static pitch angle is increased, as highlighted in Table 6, where the static pitch angles 5°–Case A, 7°–Case B and 10°–Case C yielded reduced platform masses, respectively. The reduction in the platform's mass based on design and optimization constraints leads to a reduction in the total cost of the wind farm as subsequently discussed in this section. The reduction in the masses of the platform as the static pitch angle increases is a key finding in this study, as the focus is on the platform. While it is economically viable with the reduction in mass of the platform due to less expenditure on the steel required for manufacturing the floaters, smaller platform mass at larger static pitch angles can yield excessive stress at the base of the tower, thereby causing increased fatigue damage, as highlighted in [51].

The estimations of the costs and assumptions made based on references from the literature are presented in Table 7, while the total cost estimate for the hypothetical 30 MW Hywind site based on the variation in cost of the platform due to the static pitch angles are presented in Table 8. Similarly, a sensitivity study is conducted for a larger FOWF site–60 MW farm to assess the total cost estimate for the OC3 platform and the optimal design variants based on the selected constraints and data presented in Table A1 of Appendix A.

A clear trend in results from Table 8 shows that the Hywind farm with the OC3 platform has the largest total cost. This is partly due to the observation made in [56] that the OC3 spar floater is highly over-dimensioned for safety reasons; hence, more material cost for the platform, which impacts the total cost of the wind farm, as highlighted in Table 8. The total cost estimates of the FOWFs in Table 8 from the third column to the fifth column show that the static pitch angle (5°, 7° and 10°) constraints used within the design and optimization framework highlighted in Section 3.2 have the capacity to reduce or increase the mass of the optimal design variant. The increase or decrease in the mass of the optimal platform's design variant is proportional to an increase or decrease in the cost of steel material for the platform, and a cumulative effect of the cost increase or decrease is seen in as the FOWF highlighted in Table 8. The same observation is made on a larger

FOWF, i.e., the larger the static pitch angle, the smaller the mass of the platform and hence the total cost of material, which significantly contributes to the total cost of the farm. The impact of the static pitch angle design constraints on the LCOE of the farm is discussed in Section 3.3.2.

Table 6. Platform mass and corresponding cost estimate.

Platform Type	Mass (Tonnes)	Cost-Steel (GBP)
OC3	1069.86	1.50×10^6
Case A	811.29	1.14×10^6
Case B	781.84	1.09×10^6
Case C	736.55	1.03×10^6

Table 7. Assumptions for hypothetical Hywind wind farm (30 MW–6 Turbines).

CAPEX Components	Assumption	Unit	Reference
Turbine	1.3	[million GBP/MW]	[29]
Platform	Material cost.f	[million GBP]	[29,55]
Anchors	80,000/Anchor	[GBP]	[54]
Moorings	500	[GBP/m]	[57]
Export marine cables	400	[GBP/m]	[29]
Array marine cables	600	[GBP/m]	[29,55]
Installation	1.5	[m GBP/MW]	[54]
Offshore electrical substation	3,312,000	[million GBP]	Scaled from Maienza, Avossa, Ricciardelli, Coiro, Troise and Georgakis [55]
Onshore electrical substation	1,653,600	[million GBP]	Scaled from Maienza, Avossa, Ricciardelli, Coiro, Troise and Georgakis [55]
OPEX			
Operating Expenditure	19% of Total Expenditure		[55]
DECEX			
Decommissioning and clearing	4% of Total Expenditure		[55]

Table 8. Total cost for hypothetical Hywind wind farm (30 MW–6 Turbines).

	OC3 Platform	5° Static Pitch Angle Platform-CaseA	7° Static Pitch Angle Platform-CaseB	10° Static Pitch Angle Platform-CaseC
CAPEX Estimate (GBP)	171,063,720	160,203,780	158,966,880	157,084,700
OPEX Estimate (GBP)	42,210,528	39,530,803	39,225,594	38,756,225
DECEX Estimate (GBP)	8,886,427	8,322,274	8,258,020	8,159,205
Total Cost (GBP)	222,160,675	208,056,857	206,450,494	203,980,130

3.3.2. LCOE Estimation

The LCOE is a method used to obtain the cost of one unit of energy produced and is typically applied to compare the cost competitiveness of different power generation technologies and concepts [22]. LCOE results are based on the discounted values of CAPEX, OPEX and DECEX before being distributed relative to the energy generation [57].

The discount rate is a critical criterion in estimating the LCOE, as a higher discount rate indicates a larger LCOE value while a lower discount rate implies a smaller LCOE value in the future [58]. The discount rate typically presents values in the range of 8–12% for offshore wind investments [31]. For conservative purposes, this study is adopting a discount rate of 10% and the lifetime of the project is set to be 20 years.

The CAPEX values for this study are distributed as per the values in Table 8 for the 30 MW demonstration wind farm for the four varying optimal platform designs considered, and in Table A1 of Appendix A for the 60 MW demonstration project considered for the different optimal platform designs considered. The OPEX costs are assumed to be evenly distributed over the 20 years of operation. The DECEX cost is assumed to be a one-off distribution process after the operation phase.

The mass of the designed platform tends to vary based on the design constraint specified, as highlighted in Table 4 and shown in Figure A1 of Appendix B, where the mass of the optimal platform variants reduces as the static pitch angle constraint is increased. The cumulative effect of the reduction in mass due to the design constraint on the total cost of the farm is discussed in Section 3.3.1. However, the cumulative effect of the reduction in mass due to design constraints on the platform cost for a 30 MW farm and a 60 MW farm are highlighted in Table 9 and shown in Figures A2 and A4, respectively, of Appendix B. Table 9 shows that for both the 30 MW and 60 MW FOWFs, the total mass of the platforms used in both sides reduces as the static pitch angles are increased from 5° to 7° and 10° respectively for both FOWFs. This reduction in the mass of steel used in manufacturing the designed platforms also culminates in a reduction in the cost of the materials used in manufacturing the platforms as detailed in Table 9 for both FOWFs.

Table 9. Estimated total platform mass and total platform material cost for 30 MW and 60 MW FOWF.

Design Variants	30 MW FOWF Platform Mass (Tonnes)	60 MW FOWF Platform Mass (Tonnes)	30 MW FOWF Platform Cost (£)	60 MW FOWF Platform Cost (£)
OC3 Design	6419.16	12,838.32	8.99×10^6	1.80×10^7
Case A-5° Static Pitch angle	4867.74	9735.48	6.81×10^6	1.36×10^7
Case B-7° Static Pitch angle	4691.04	9382.08	6.57×10^6	1.31×10^7
Case C-10° Static Pitch angle	4419.3	8838.6	6.19×10^6	1.24×10^7

The LCOE for the 30 MW site and the 60 MW site is developed based on the site's total costs for each optimal design highlighted in Section 3.3.1 and Appendix A, respectively. This study investigates the LCOE result from two fronts highlighted below:

1. The impact of the design constraint on the estimated LCOE of the FOWF.
2. The effect of scaling up a FOWF on the LCOE of the project.

The impact of the design constraint—mainly the static pitch angle on the LCOE—is demonstrated on a 30 MW FOWF as highlighted in Table 10. In assessing this impact, the OC3 model is the base model, while the percentage difference on the 5°, 7° and 10° static pitch angle constraint-optimized design variants are measured relative to the OC3 base model. Table 10 shows that the LCOE of the optimized variants relative to the OC3 base model is reduced by 6.34%, 7.07% and 8.18% for the 5°, 7° and 10° static pitch angle constraint optimized design variants respectively. Similarly, for the 60MW FOWF, Table 11 shows that the corresponding LCOE of the optimized variants relative to the OC3 base model is reduced by 4.81%, 5.58% and 6.76% for the 5°, 7° and 10° static pitch angle constraint optimized design variants, respectively. This shows the potential of reducing the LCOE in FOWFs by varying the static pitch angle constraints.

Table 10. LCOE comparison for 30 MW OC3 base model and 5°, 7° and 10° Static Pitch angle constrained optimized models.

Design Variants	LCOE–30 MW FOWF (£/MWh)	Design Variants	LCOE–30 MW FOWF (£/MWh)	Percentage Difference (%)
OC3 Design	197	Case A-5° Static Pitch angle	185	6.34
OC3 Design	197	Case B-7° Static Pitch angle	183	7.07
OC3 Design	197	Case C-10° Static Pitch angle	181	8.18

Table 11. LCOE comparison for 60 MW OC3 base model and 5°, 7° and 10° Static Pitch angle constrained optimized models.

Design Variants	LCOE–30 MW FOWF (£/MWh)	Design Variants	LCOE–30 MW FOWF (£/MWh)	Percentage Difference (%)
OC3 Design	185	Case A-5° Static Pitch angle	176	4.81
OC3 Design	185	Case B-7° Static Pitch angle	175	5.58
OC3 Design	185	Case C-10° Static Pitch angle	173	6.76

The study on the effect of scaling up the 30 MW FOWF is conducted by doubling its capacity to 60 MW. The LCOE results for the 30 MW and 60 MW FOWF are highlighted in Table 12. The LCOE for the 60 MW OC3 platform FOWF is 6.23% lower than the LCOE of the 30 MW OC3 platform FOWF. Similarly, the 5°, 7° and 10° static pitch angle constraint design variants of the 60 MW FOWF are 4.68%, 4.72% and 4.78% lower in LCOE value than the corresponding optimal design variants for the 30 MW FOWF.

Table 12. LCOE comparison for 30 MW and 60 MW FOWF with 10% discount rate.

Design Variants	LCOE–30 MW FOWF (£/MWh)	LCOE–60 MW FOWF (£/MWh)	Percentage Difference (%)
OC3 Design	197	185	6.23
Case A-5° Static Pitch angle	185	176	4.68
Case B-7° Static Pitch angle	183	175	4.72
Case C-10° Static Pitch angle	181	173	4.78

This significant reduction in LCOE values between the 60 MW FOWF and the 30 MW FOWF is a cumulative effect of the mass optimization of the platform as detailed in Section 3.2 and the concept of scaling up the floating wind size (economies of scale). The concept of increasing the farm size is detailed in [57], where they showed that increasing the number of turbines from 100 to 200 would lower the LCOE by approximately 10% and that increasing the turbines to 600 results in an LCOE reduction of up to 15%. The reduction in the LCOE value for the optimal design variants between the 60 MW and 30 MW FOWFs considered in this study is less than 5%. The 5% reduction in LCOE value is not as significant as the 10% to 15% reduction in LCOE value recorded in M [57]. However, comparing the number of turbines, 200, it took Myhr et al. [57] to attain 10% reduction in LCOE value with the 12 turbines we have used to attain about 5% reduction in LCOE value in this study, the approach adopted using platform mass optimization in combination with

scaling up the floating wind farm is a much more effective approach to reducing the value of the LCOE in comparison to just scaling up the farm size or conducting platform mass optimization alone.

4. Conclusions and Recommendations

This study investigates the economic implications of the use of bespoke geometric shape parameterization, design, analysis and optimization framework of spar platforms on a 30 MW floating wind farm and also the cumulative effect of this bespoke approach and economies of scale on a 60 MW floating wind farm. While the mesoscale impact of the sea surface on offshore wind farms' wind patterns and resources is important in estimating the AEP, and invariably the LCOE, the focus here is on the platform, which contributes significantly to the capital cost of the LCOE. The bespoke technical assessment was conducted using the B-spline shape parameterization technique within an optimization framework to design, analyze and optimize the concept. The shape parameterization and alteration of the design was conducted with Sesam Genie using the B-spline parameterization technique. Analysis of the design was conducted using the hydrostatic capability of the Hydro D tools and optimization of the framework was executed with the Pattern search (derivative-free) optimization method. The main design constraint within the optimizer to facilitate the shape alteration within the optimization framework is the static pitch angle. This study considered three static pitch angles of 5°, 7° and 10°, respectively, and the OC3 NREL model. As highlighted in the literature, the OC3 model is over-dimensioned for safety reasons; hence, it has the largest mass of all the optimal models considered. It is followed by the 5° static pitch angled optimal model, then by the 7° and 10° static pitch angled optimal models, respectively. This shows that, as the static pitch angle is increased, the mass of the optimal platform model reduces. The mass reduction in the platform as a result of the constraints used in the design contributes to a reduction in material cost, a vital component of the total CAPEX cost for a FOWF.

The ratio of the net present value of total cost to the net present value of electricity generation, which translates to the LCOE, are the financial parameters used in assessing the different scenarios considered in this study (30 MW FOWFs and 60 MW FOWFs for OC3 NREL platforms, 5°, 7° and 10° static pitch constrained platforms). The LCOE values for the 30 MW FOWFs based on the OC3 platform model and static pitch constraints platform models of 5°, 7° and 10° are 197 £/MWh, 185 £/MWh, 183 £/MWh and 181 £/MWh, respectively. On scaling up the farm size to 60 MW, the estimated LCOE values for the 30 MW FOWFs based on the OC3 platform model and static pitch constraints platform models of 5°, 7° and 10° are 185 £/MWh, 176 £/MWh, 175 £/MWh and 173 £/MWh respectively, which is 6.23%, 4.68%, 4.72% and 4.78% lower than the corresponding optimal design variants for the 30 MW FOWF. This is due to a combination of design shape parameterization and optimization framework utilized in this study and economy of scale.

Recommended future work from this study is the structural assessment of the bespoke shaped optimized spar subject to different environmental conditions, as it has been highlighted in some work that increasing the static pitch angle tends to have consequences for the fatigue life of the tower. Manufacturing of a bespoke-shaped spar is a constraint that must not be overlooked. However, ongoing research in the advancement of wire arc additive manufacturing (WAAM), particularly in the 3D printing of metals, and the development of concrete slip-forming techniques are expected to potentially provide valuable solutions for overcoming this constraint.

This preliminary study shows that, in addition to other means of ensuring FOWT technology is as economically and technically viable as its fixed-bottom counterpart (platform upscaling, government subsidy, holistic system MDAO), geometric shape design and optimization of FOWT platform is an effective method that can be used in reducing the cost of floating wind farms.

Author Contributions: Article structure and conceptualization, A.O., M.C. and A.C.; Design and shape alteration Software A.O.; Data curation, A.O.; Optimization framework, A.O., M.C. and A.C.; Analyses and Investigation, A.O. and M.C.; Writing—Original draft preparation, A.O.; Writing—review and editing, M.C. and A.C.; Project Supervision, M.C. and A.C. All authors have read and agreed to the published version of the manuscript.

Funding: This work is conducted with the Renewable Energy Marine Structures (REMS) group at the University of Strathclyde and the funding is provided by the Engineering and Physical Sciences Research Council (EPSRC) UK (Grant no: EP/L016303/1).

Data Availability Statement: The original contributions presented in the study are included in the article, further inquiries can be directed to the corresponding author.

Conflicts of Interest: The contact author declared that none of the authors has any competing interests.

Abbreviations

AEP	Annual Energy Production
B-Spline	Basis Spline
CAPEX	Capital Expenditure
DECEX	Decommissioning Expenditure
DPBP	Discounted Pay Back Period
DNV	Det Norske Veritas
GBP	Great British Pounds
GWh	Giga Watts Hour
FOWF	Floating Offshore Wind Farm
FOWT	Floating Offshore Wind Turbine
IRR	Internal Rate of Returns
LCOE	Levelized Cost of Energy
MDAO	Multidisciplinary Design Analysis and Optimization
MW	Mega Watts
MWh	Mega Watts Hour
MSL	Mean Sea Level
NPV	Net Present Value
OC3	Offshore Code Comparison Collaboration
OPEX	Operating Expenditure
OWT	Offshore Wind Turbine
PSM	Pattern Search Model
TLP	Tension-Leg Platform
WACC	Weighted Average Capital Cost
WADAM	Wave Analysis by Diffraction and Morison Theory

Appendix A

This appendix provides total estimated cost for the scaled up Hywind wind farm from 30 MW to 60 MW highlighting the variation in total costs due to the design constraint as discussed in Section 3.

Table A1. Total cost for scaled up Hywind wind farm (60 MW–12 Turbines).

	OC3 Platform	**5° Static Pitch Angle Platform-CaseA**	**7° Static Pitch Angle Platform-CaseB**	**10° Static Pitch Angle Platform-CaseC**
CAPEX Estimate (GBP)	320,827,440	305,407,560	302,933,760	299,129,400
OPEX Estimate (GBP)	79,165,213	75,360,307	74,749,889	73,811,151
DECEX Estimate (GBP)	16,666,361	15,865,328	15,736,819	15,539,190
Total Cost (GBP)	416,659,013	396,633,195	393,420,468	388,479,740

Appendix B

This appendix provides total estimated mass for each optimized platform and the base design in Figure A1, which shows the total mass for each floating platform variant; Figures A2 and A4 show the total platform steel cost for the 30 MW FOWF and 60 MW FOWF, respectively. Figures A3 and A5 show the LCOE and total platform steel cost for the 30MW FOWF and 60MW FOWF, respectively.

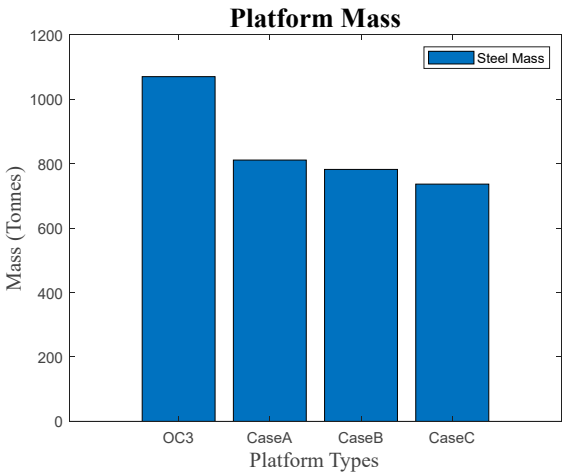

Figure A1. Mass of platform types.

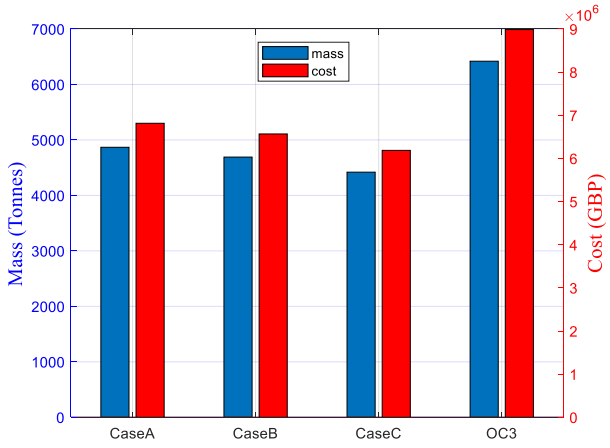

Figure A2. 30MW Farm Total Platform Mass and Total Platforms Steel Cost.

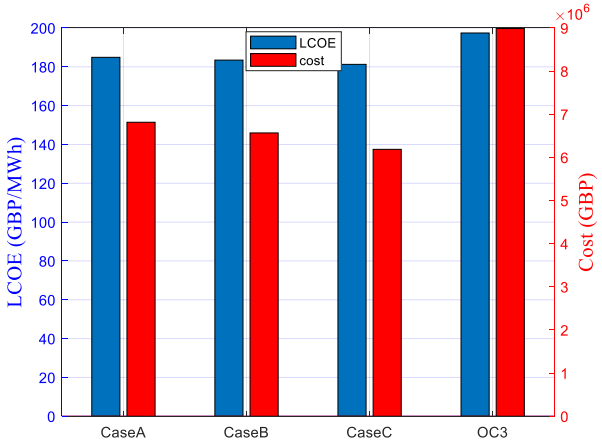

Figure A3. 30MW Farm LCOE and Total Platforms Steel Cost.

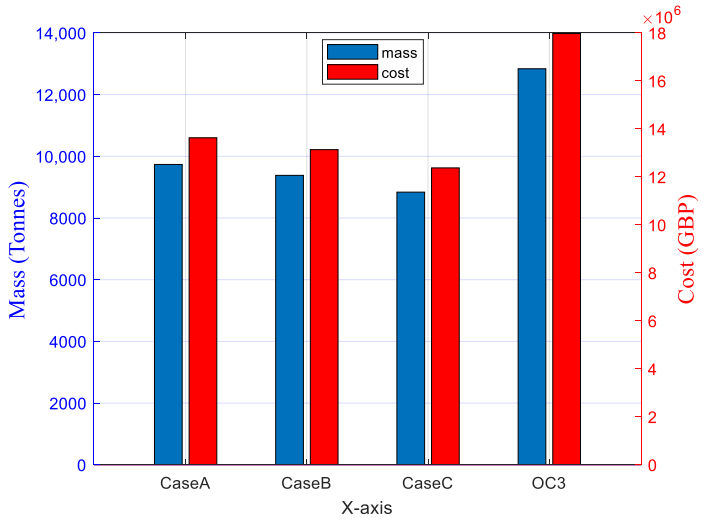

Figure A4. 60MW Farm Total Platform Mass and Total Platforms Steel Cost.

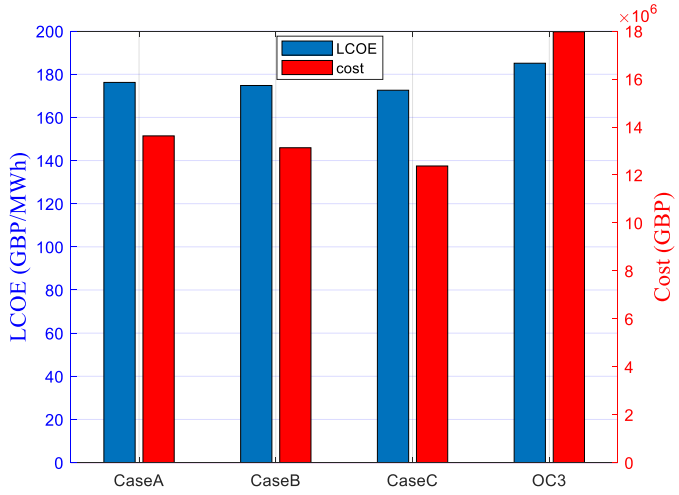

Figure A5. 60MW Farm LCOE and Total Platforms Steel.

References

1. GWEC. *Floating Offshore Wind—A Global Opportunity*; Global Wind Energy Council: Brussels, Belgium, 2022.
2. DNV-GL. *Floating Wind: The Power to Commercialize*; DNV: Oslo, Norway, 2020.
3. Heronemus, W.E. Pollution-free energy from the offshore winds. In Proceedings of the 8th Annual Conference and Exposition, Marine Technology Society, Washington, DC, USA, 11–13 September 1972.
4. Zheng, X.Y.; Lei, Y. Stochastic response analysis for a floating offshore wind turbine integrated with a steel fish farming cage. *Appl. Sci.* **2018**, *8*, 1229. [CrossRef]
5. Ramachandran, C.R.; Desmond, C.; Judge, F.; Serraris, J.-J.; Murphy, J. Floating offshore wind turbines: Installation, operation, maintenance and decommissioning challenges and opportunities. *Wind Energy Sci. Discuss* **2021**, *2021*, 15.
6. Kaldellis, J.K.; Apostolou, D.; Kapsali, M.; Kondili, E. Environmental and social footprint of offshore wind energy. Comparison with onshore counterpart. *Renew. Energy* **2016**, *92*, 543–556. [CrossRef]
7. IRENA. *Future of Wind. Deployment, Investment, Technology, Grid Integration and Socio–Economic Aspects*; IRENA: Abu Dhabi, United Arab Emirates, 2019.
8. Butterfield, S.; Musial, W.; Jonkman, J.M.; Sclavounos, P.D. *Engineering Challenges for Floating Offshore Wind Turbines*; National Renewable Energy Lab: Golden, CO, USA, 2007.
9. Leimeister, M.; Kolios, A.; Collu, M. Critical review of floating support structures for offshore wind farm deployment. *J. Phys. Conf. Ser.* **2018**, *1104*, 012007. [CrossRef]
10. Linnenschmidt, J.-N. *Cost Comparison between Bottom-Fixed and Floating Offshore Wind Turbines-Calculating LCOE Based on Full Hours of Utilization and Corresponding Break-Even Points*; FH Münster: Münster, Germany, 2021.
11. Ioannou, A.; Liang, Y.; Jalón, M.L.; Brennan, F.P. A preliminary parametric techno-economic study of offshore wind floater concepts. *Ocean. Eng.* **2020**, *197*, 106937. [CrossRef]

12. Clauss, G.F.; Birk, L. Hydrodynamic shape optimization of large offshore structures. *Appl. Ocean. Res.* **1996**, *18*, 157–171. [CrossRef]
13. Birk, L.; Clauss, G. Parametric hull design and automated optimization of offshore structures. In Proceedings of the 10th Int. Congress of the Int. Maritime Association of the Mediterranean, Hellas, Greece, 13–17 May 2002.
14. Birk, L. Parametric modeling and shape optimization of offshore structures. *Int. J. CAD/CAM* **2006**, *6*, 29–40.
15. Ojo, A.; Collu, M.; Coraddu, A. Multidisciplinary design analysis and optimization of floating offshore wind turbine substructures: A review. *Ocean. Eng.* **2022**, *266*, 112727. [CrossRef]
16. Leimeister, M.; Bachynski, E.E.; Muskulus, M.; Thomas, P. Rational Upscaling of a Semi-submersible Floating Platform Supporting a Wind Turbine. *Energy Procedia* **2016**, *94*, 434–442. [CrossRef]
17. Kikuchi, Y.; Ishihara, T. Upscaling and levelized cost of energy for offshore wind turbines supported by semi-submersible floating platforms. *J. Phys. Conf. Ser.* **2019**, *1356*, 012033. [CrossRef]
18. Papi, F.; Bianchini, A. Technical challenges in floating offshore wind turbine upscaling: A critical analysis based on the NREL 5 MW and IEA 15 MW Reference Turbines. *Renew. Sustain. Energy Rev.* **2022**, *162*, 112489. [CrossRef]
19. Leimeister, M.; Kolios, A.; Collu, M. Development and Verification of an Aero-Hydro-Servo-Elastic Coupled Model of Dynamics for FOWT, Based on the MoWiT Library. *Energies* **2020**, *13*, 1974. [CrossRef]
20. Karimi, M.; Hall, M.; Buckham, B.; Crawford, C. A multi-objective design optimization approach for floating offshore wind turbine support structures. *J. Ocean. Eng. Mar. Energy* **2017**, *3*, 69–87. [CrossRef]
21. Karimi, M. Frequency Domain Modeling and Multidisciplinary Design Optimization of Floating Offshore Wind Turbines. Ph.D. Thesis, University of Victoria, Victoria, BC, Canada, 2018.
22. Lerch, M.; Norbeck, J.A.; Berthelsen, P.A. Life50+: D2.8 Expected LCOE for Floating Wind Turbines 10MW+ for 50m+ Water Depth; 2019. Available online: https://ec.europa.eu/research/participants/documents/downloadPublic?documentIds=080166e5c3ac71f4&appId=PPGMS (accessed on 15 April 2024).
23. Farin, G. *Curves and Surfaces for Computer-Aided Geometric Design*; Academic Press: New York, NY, USA, 1990.
24. Birk, L.; Clauss, G.F.; Lee, J.Y. Practical application of global optimization to the design of offshore structures. In Proceedings of the International Conference on Offshore Mechanics and Arctic Engineering, St. John's, NF, Canada, 11–16 July 1999; pp. 567–579.
25. Hegseth, J.M.; Bachynski, E.E.; Martins, J.R. Integrated design optimization of spar floating wind turbines. *Mar. Struct.* **2020**, *72*, 102771. [CrossRef]
26. Maienza, C.; Avossa, A.M.; Picozzi, V.; Ricciardelli, F. Feasibility analysis for floating offshore wind energy. *Int. J. Life Cycle Assess.* **2022**, *27*, 796–812. [CrossRef]
27. IRENA. *Renewable Power Generation Costs in 2018*; IRENA: Abu Dhabi, United Arab Emirates, 2019.
28. Ojo, A.; Collu, M.; Coraddu, A. Parametrisation Scheme for Multidisciplinary Design Analysis and Optimisation of a Floating Offshore Wind Turbine Substructure—OC3 5MW Case Study. *J. Phys. Conf. Ser.* **2022**, *2265*, 042009. [CrossRef]
29. Ghigo, A.; Cottura, L.; Caradonna, R.; Bracco, G.; Mattiazzo, G. Engineering: Platform Optimization and Cost Analysis in a Floating Offshore Wind Farm. *Mar. Sci. Eng.* **2020**, *8*, 835. [CrossRef]
30. Castro-Santos, L.; Martins, E.; Guedes Soares, C. Cost assessment methodology for combined wind and wave floating offshore renewable energy systems. *Renew. Energy* **2016**, *97*, 866–880. [CrossRef]
31. Martinez, A.; Iglesias, G. Mapping of the levelised cost of energy for floating offshore wind in the European Atlantic. *Renew. Sustain. Energy Rev.* **2022**, *154*, 111889. [CrossRef]
32. Filgueira-Vizoso, A.; Castro-Santos, L.; Iglesias, D.C.; Puime-Guillén, F.; Lamas-Galdo, I.; García-Diez, A.I.; Uzunoglu, E.; Díaz, H.; Soares, C.G. The Technical and Economic Feasibility of the CENTEC Floating Offshore Wind Platform. *J. Mar. Sci. Eng.* **2022**, *10*, 1344. [CrossRef]
33. Pham, T.D.; Shin, H. A New Conceptual Design and Dynamic Analysis of a Spar-Type Offshore Wind Turbine Combined with a Moonpool. *Energies* **2019**, *12*, 3737. [CrossRef]
34. Campos, A.; Molins, C.; Gironella, X.; Trubat, P. Spar concrete monolithic design for offshore wind turbines. *Proc. Inst. Civ. Eng. -Marit. Eng.* **2016**, *169*, 49–63. [CrossRef]
35. Lerch, M.; De-Prada-Gil, M.; Molins, C.; Benveniste, G. Sensitivity analysis on the levelized cost of energy for floating offshore wind farms. *Sustain. Energy Technol. Assess.* **2018**, *30*, 77–90. [CrossRef]
36. Castro-Santos, L.; Bento, A.R.; Silva, D.; Salvação, N.; Guedes Soares, C. Economic Feasibility of Floating Offshore Wind Farms in the North of Spain. *J. Mar. Sci. Eng.* **2020**, *8*, 58. [CrossRef]
37. Hall, M.; Buckham, B.; Crawford, C. Evolving offshore wind: A genetic algorithm-based support structure optimization framework for floating wind turbines. In Proceedings of the OCEANS 2013 MTS/IEEE Bergen: The Challenges of the Northern Dimension, Bergen, Norway, 10–13 June 2013; pp. 1–10.
38. Dou, S.; Pegalajar-Jurado, A.; Wang, S.; Bredmose, H.; Stolpe, M. Optimization of floating wind turbine support structures using frequency-domain analysis and analytical gradients. *J. Phys. Conf. Ser.* **2020**, *1618*, 042028. [CrossRef]
39. Castro-Santos, L.; Silva, D.; Bento, A.R.; Salvação, N.; Guedes Soares, C. Economic feasibility of floating offshore wind farms in Portugal. *Ocean. Eng.* **2020**, *207*, 107393. [CrossRef]
40. Wu, C.; Wang, Q.; Luo, K.; Fan, J. Mesoscale impact of the sea surface on the performance of offshore wind farms. *J. Clean. Prod.* **2022**, *372*, 133741. [CrossRef]

41. Ramachandran, G.; Robertson, A.; Jonkman, J.; Masciola, M.D. Investigation of response amplitude operators for floating offshore wind turbines. In Proceedings of the Twenty-Third International Offshore and Polar Engineering Conference, Ottawa, ON, Canada, 19–23 June 2023.
42. Munir, H.; Lee, C.F.; Ong, M.C. Global analysis of floating offshore wind turbines with shared mooring system. *IOP Conf. Ser. Mater. Sci. Eng.* **2021**, *1201*, 012024. [CrossRef]
43. Collu, M.; Borg, M. Design of floating offshore wind turbines. In *Offshore Wind Farms: Technologies, Design and Operation*; Elsevier Inc.: Amsterdam, The Netherlands, 2016; pp. 359–385.
44. Shields, M.; Duffy, P.; Musial, W.; Laurienti, M.; Heimiller, D.; Spencer, R.; Optis, M. *The Costs and Feasibility of Floating Offshore Wind Energy in the O'ahu Region*; NREL: Golden, CO, USA, 2021.
45. Jonkman, J.M. *Definition of the Floating System for Phase IV of OC3*; NREL: Golden, CO, USA, 2010.
46. Riesenfeld, R. Applications Of B-Spline Approximation to Geometric Problems of Computer-Aided Design. In *Electrical Engineering and Computer Science—Dissertations and Theses*; Syracuse University: Syracuse, NY, USA, 1973.
47. Samareh, J.A. Survey of shape parameterization techniques for high-fidelity multidisciplinary shape optimization. *AIAA J.* **2001**, *39*, 877–884. [CrossRef]
48. Findler, N.V.; Lo, C.; Lo, R. Pattern search for optimization. *Math. Comput. Simul.* **1987**, *29*, 41–50. [CrossRef]
49. Anaya-Lara, O.; Tande, J.O.; Uhlen, K.; Merz, K. *Offshore Wind Energy Technology*; John Wiley & Sons: Hoboken, NJ, USA, 2018.
50. Bachynski, E.E.; Collu, M. Offshore support structure design. In *Renewable Energy from the Oceans: From Wave, Tidal and Gradient Systems to Offshore Wind and Solar*; Institution of Engineering and Technology: London, UK, 2019; pp. 271–319. [CrossRef]
51. Souza, C.E.S.d.; Bachynski-Polić, E.E. Design, structural modeling, control, and performance of 20 MW spar floating wind turbines. *Mar. Struct.* **2022**, *84*, 103182. [CrossRef]
52. Saenz-Aguirre, A.; Ulazia, A.; Ibarra-Berastegi, G.; Saenz, J. Floating wind turbine energy and fatigue loads estimation according to climate period scaled wind and waves. *Energy Convers. Manag.* **2022**, *271*, 116303. [CrossRef]
53. Aldersey-Williams, J.; Broadbent, I.D.; Strachan, P.A. Analysis of United Kingdom offshore wind farm performance using public data: Improving the evidence base for policymaking. *Util. Policy* **2020**, *62*, 100985. [CrossRef]
54. James, R.; Ros, M.C. Floating Offshore Wind: Market and Technology Review. *Carbon Trust* **2015**, *439*, 79–93.
55. Maienza, C.; Avossa, A.M.; Ricciardelli, F.; Coiro, D.; Troise, G.; Georgakis, C.T. A life cycle cost model for floating offshore wind farms. *Appl. Energy* **2020**, *266*, 114716. [CrossRef]
56. Leimeister, M.; Kolios, A.; Collu, M.; Thomas, P. Design optimization of the OC3 phase IV floating spar-buoy, based on global limit states. *Ocean. Eng.* **2020**, *202*, 107186. [CrossRef]
57. Myhr, A.; Bjerkseter, C.; Ågotnes, A.; Nygaard, T.A. Levelised cost of energy for offshore floating wind turbines in a life cycle perspective. *Renew. Energy* **2014**, *66*, 714–728. [CrossRef]
58. Aldersey-Williams, J.; Rubert, T. Levelised cost of energy—A theoretical justification and critical assessment. *Energy Policy* **2019**, *124*, 169–179. [CrossRef]